Spatiotemporal intermittency and scaling laws in coupled map lattices

Neelima Gupte[1] and Zahera Jabeen[2]

Department of Physics, IIT Madras, Chennai 600036, India.

Abstract

We discuss the spatiotemporal intermittency (STI) seen in coupled map lattices (CML-s). We identify the types of intermittency seen in such systems in the context of several specific CML-s. The Chaté-Manneville CML is introduced and the on-going debate on the connection of the spatiotemporal intermittency seen in this model with the problem of directed percolation is summarised. We also discuss the STI seen in the sine circle map model and its connection with the directed percolation problem, as well as the inhomogenous logistic map lattice which shows the novel phenomenon of spatial intermittency and other types of behaviour not seen in the other models. The connection of the bifurcation behaviour in this model with STI is touched upon. We conclude with a discussion of open problems.

1   Introduction

Regimes of spatiotemporal intermittency, wherein laminar regions, which exhibit regular dynamics in space and time, coexist and propagate together with regions which show irregular or chaotic bursts, can be seen in a wide variety of spatially extended systems in the laboratory as well as in theoretical model systems. Such regimes have been regarded as precursors to regimes of fully developed spatiotemporal chaos [1]. Spatiotemporal intermittent behaviour has been seen in theoretical models such as coupled map lattices [2, 3], probabilistic cellular automata [4], and

partial differential equations [5, 6], as well as in experimental systems such as chemical reactions [7], Rayleigh-Benard convection in narrow channels and annuli [8, 9], planar Couette flow [10], studies of fluid flows between rotating eccentric cylinders such as the Taylor-Dean [11] and Taylor-Couette [12, 13] flows, and the 'printer's instability' [14]. A variety of scaling laws have been observed in these systems. However, there are no definite conclusions about their universal behaviour. Many of the observed phenomena have been seen in experimental systems where no simple model is available. There is a lively on-going debate about the nature of spatiotemporal intermittency and its analogy with systems which undergo phase transitions. Thus, the analysis of spatiotemporal intermittency remains a challenging theoretical problem. In this review, we will concentrate on spatiotemporal intermittency in coupled map lattices, i.e. systems with continuous variables which evolve on discrete space-time.

Spatiotemporally intermittent behavior has been divided into two classes. In the first type, there is no spontaneous creation of bursts. Under spatial coarse-graining, if a site and its neighbours show laminar behaviour at a given step, the site remains laminar at the next time step. However it can show turbulent behaviour if infected by a turbulent neighbour. A turbulent site can either relax to laminar behaviour or infect its neighbour. Below a threshold parameter, which controls the propagation rate of turbulence, the turbulence dies out. Once the whole system reaches the laminar state, it has no way of escaping from this state. Hence the laminar state is called the absorbing state. Above the threshold parameter, the turbulence spreads over the whole lattice. Thus the burst states 'percolate' through space-time. It has therefore been argued that the transition to this type of spatiotemporal intermittency is a second order phase transition, and that this transition falls in the same universality class as directed percolation [15] with the laminar states being identified with the 'inactive' states and the turbulent states being identified as the 'active' or

percolating states. This conjecture has become the central issue in a long-standing debate [16, 17, 18, 19, 20], which is still not completely resolved.

In the second type of intermittency, the spontaneous creation of bursts can be seen, given some coarse-grained reduction of the states. Thus, for this case, a laminar site has a finite probability of undergoing a turbulent burst even if all its neighbours are laminar. This kind of intermittency is associated with the transition of a spatial pattern. A typical example of this type of intermittency is observed in the coupled logistic lattice from pattern selection to fully developed spatiotemporal chaos [2] as well as in experiments on Benard convection [8, 9], Faraday instabilities [21], and in two-dimensional electric convection in a liquid crystal [22].

2 The Chaté-Manneville map and its variants:

The conjecture by Pomeau that the transition to spatiotemporal intermittency of the first type with a laminar absorbing state belongs to the same universality class as directed percolation has been very extensively investigated. A very simple coupled map model was introduced by Chaté and Manneville for the investigation of this conjecture.

The Chaté-Manneville maps at different sites are coupled together by linear diffusive coupling of the form

$$x^{n+1}(i) = (1 - \epsilon)f(x^n(i)) + \frac{\epsilon}{2}[f(x^n(i+1)) + f(x^n(i-1))] \tag{1}$$

The single site Chaté-Manneville map has the form

$$
\begin{aligned}
f(x) &= rx & 0 \leq x < 1/2 \\
&= r(1-x) & 1/2 \leq x \leq 1 \\
&= x & 1 < x \leq r/2
\end{aligned}
\tag{2}
$$

where $r > 2$. The return map is shown in Fig. 1.

The uncoupled dynamics of such a map is chaotic as long as $f(x)$ remains in the unit interval since $r > 1$ everywhere in this domain. However, as soon as $f(x) > 1$ the iteration is locked on to a fixed point. The local phase space is thus a marginally stable fixed line ($x \in [1, r/2]$), connected to a chaotic repeller ($x \in [0, 1]$). There is thus a clear and natural distinction between laminar and turbulent states for a given site. Chaté and Manneville argued that since the model has no single stable fixed point or globally attracting period, there is no additional local dynamics to complicate the transition from local transient chaos to global spatiotemporal chaos via the spatial coupling alone.

The dynamics of this chain was studied with random initial conditions. At $\epsilon > \epsilon_c$, sustained spatiotemporal intermittency was seen for the system for $r = 2.1$ and $r = 3$. The lattice showed regions of laminar behaviour punctuated by chaotic bursts (See Fig. 2). The distribution of the lengths of the laminar regions showed power-law behaviour of the form $P(l) \approx l^{-\zeta}$ with the exponent ζ taking values between 1.67 and 1.78 at $r = 2.1$ and 1.9 to 1.99 at $r = 3$.(The simulated DP values for the corresponding exponent ranged from 1.6 to 1.74). It was initially argued that the values obtained showed significant departures from the directed percolation exponents and hence that spatiotemporal intermittency did not belong to the DP universality class. However Grassberger et al examined the same CML later [19] and found that the departures from DP exponents at $r = 2.1$ were insignificant on long time-scales. In contrast, statistically significant departures from DP were observed at $r = 3.0$. It was observed that for this case, long straight lines of turbulent sites were seen in the space-time plot (Fig. 2(b)). These were called 'solitons' and were reflective of long range correlations in the system. Grassberger and Schreiber argued that these long range correlations spoilt the analogy with DP and hence led to the departure of the STI in this system from the DP universality class. The existence

of solitons led to the emergence of a length and time scale (the mean life time of the solitons) which is independent of critical fluctuations, and hence led to departures from the DP class [19]. Since the solitons in this model had very long life-times, they also conjectured that the cross-over times in this model could be very long and the real asymptotic behaviour of the model could still be in the DP universality class.

The conjecture that the solitons were the primary ingredient which spoilt DP universality was tested in a variety of ways [16, 23, 24]. The CML of eq. 2 was evolved with asynchronous up-dates i.e. the maps at every site were not updated simultaneously, but were updated one after another in a random sequence. The asynchronous updates served to destroy the solitons and good agreement with a complete set of DP exponents was obtained (see Appendix for definitions of the DP exponents and Table 1 for obtained values).

Another study introduced a deterministic extension of the Chaté-Manneville model, where the soliton properties could be tuned [23, 24]. It was seen that the role played by the solitons in the transition to turbulence was more profound than that of setting a cross-over time. They were able to change nature of the transition from second to first order.

The CML equations of this solitonic Chaté-Manneville model were

$$
\begin{aligned}
x^{n+1}(i) &= (1-\epsilon)f(x^n(i)) + \frac{\epsilon}{2}[f(x^n(i+1)) + f(x^n(i-1))] + y^n(i) \\
y^{n+1}(i) &= b(x^{n+1}(i) - x^n(i))
\end{aligned}
$$

(3)

where the function $f(x)$ is the same as that in Eq. 2. The map becomes increasingly two dimensional with increase in $|b|$. Thus if x^* is a fixed point of the old CML Eq. 2, it gets mapped to the fixed point $(x^*, 0)$ of Eq. 3. The CML thus has three adjustable parameters r, ϵ, b. The parameter r was set to 3.0 and the phase diagram in ϵ, b space was obtained. The parameter b has a large influence on the existence of

solitons. The $b = 0$ case is the original Chaté-Manneville case where there are long lived solitons (Fig. 3 (c),(d)). These life-times become even longer when $b = -0.1$ (Fig. 3(a),(b)), and the solitons only vanish when they collide with other solitons or propagate into turbulent structures (Fig. 3(e),(f)). The order parameter m which is the number of active or turbulent sites, jumps sharply as a function of $\epsilon - \epsilon_c$ as in a first order transition [23, 24]. The behaviour of m at $b = 0.0$ and $b = 0.2$ is consistent with a continuous transition with exponents that approach DP values more closely as $|b|$ increases corresponding to soliton-poor regimes (Table. 2). Thus not only does the existence of solitons spoil the analogy of spatiotemporal intermittency with DP, but it can change the order of the transition itself. Thus, in order to obtain a clean comparison between directed percolation and spatiotemporal intermittency, it is desirable to examine a deterministic system which is free of coherent propagating structures. We describe such a system in the next section.

3   The sine circle coupled map lattice:

The sine circle map lattice is defined by

$$\theta^{n+1}(i) = (1 - \epsilon)f(\theta^n(i)) + \frac{\epsilon}{2}[f(\theta^n(i+1)) + f(\theta^n(i-1))] \quad (mod \ 1) \qquad (4)$$

with periodic boundary conditions. The local map is the sine circle map

$$f(\theta^n) = \theta^n + \Omega - \frac{K}{2\pi}\sin(2\pi\theta^n) \qquad (5)$$

Here, K is the strength of nonlinearity, Ω is the frequency of each single sine circle map and, ϵ is the coupling strength. This system is a popular model for the behaviour of mode-locked oscillators. The system shows regimes of spatiotemporal intermittency at certain points in the parameter space when random initial conditions are evolved synchronously. The phase diagram of the system at $K = 1$ is

shown in Fig. 4 and the points where spatiotemporal intermittency are seen are marked with diamonds [20] and pluses [25]. This system shows a transition to spatiotemporal intermittency in the presence of two types of absorbing states. The two qualitatively distinct absorbing regions are as follows [20].

(i) When the nonlinearity parameter $K = 1$, there are regions of $(\epsilon - \Omega)$ space where the system goes to the synchronised spatiotemporal fixed point $\theta^\star = \frac{1}{2\pi} \sin^{-1}(\frac{2\pi\Omega}{k})$. This constitutes an unique absorbing state. The critical behaviour was examined at 2 critical points in this regime: $\Omega = 0.064, \epsilon = 0.63775$, and $\Omega = 0.068, \epsilon = 0.73277$. These mark the transition from a laminar phase to STI. The turbulent sites here are those which are different from $\theta^\star$.

(ii) When the nonlinearity parameter $K = 3.1$, there are regions of $(\epsilon - \Omega)$ space where sites with any value less than $1/2$ constitute the absorbing states, and sites whose values are greater than $1/2$ constitute the turbulent states. The absorbing states are now infinitely many, as also weakly chaotic. The critical behaviour was examined at 2 critical points in this regime as well: $\Omega = 0.18, \epsilon = 0.701$, and $\Omega = 0.19, \epsilon = 0.65612$.

The exponents for the onset of spatiotemporal intermittency have been defined both for the bulk critical exponents and the spreading exponents (See Tables 3 and 4). In both cases there is good agreement with DP values [26]. Thus the coupled sine circle map constitutes a deterministic system evolving under synchronous updates where DP exponents are straight-forwardly obtained. There are no long-lived coherent structures at any of the parameter values where the system has been studied to spoil the analogy with DP. This also lends credence to the argument that it is the solitons which lead to the departure of the Chaté-Manneville exponents from the DP class. Certain parameter regions of the sine circle map model show regimes of spatiotemporal intermittency which is unlike the DP behaviour. These are currently under investigation. Such regimes have been seen earlier in a coupled map model

which we will discuss below.

4   The inhomogeneous logistic map lattice:

The specific system studied by us consists of an inhomogeneous lattice of coupled maps where the inhomogeneity appears in the form of different values of map parameter at different sites. Such lattices have been considered in the case of pinning studies [28]. The coupling between maps is diffusive and nearest neighbour. We consider the simplest case, that is, a situation where neighbouring lattice sites have different values of the parameter and alternate sites have the same value of the parameter.

This model is defined by the evolution equations

$$x^{n+1}(2i) = (1 - \epsilon)f(x^n(2i), \mu) + \frac{\epsilon}{2}[f(x^n(2i - 1), \mu') + f(x^n(2i + 1), \mu')] \quad (6)$$

where $f(x) = \mu x(1 - x)$ is the logistic map and μ, $\mu' \in [0, 4]$, $x^n(2i)$ is the value of the variable x at the even lattice site $2i$ at time n, and $0 \leq x \leq 1$. In the case of $x^n(2i + 1)$, the variable defined at odd lattice sites, the evolution equation is defined by the evolution above with $2i$ being replaced by $2i + 1$ and μ and μ' interchanged. We set $\mu' = \mu - \gamma$ and use periodic boundary conditions where $2N$, the number of lattice sites is even. The synchronised fixed points of the system are given by $x^* = 0$ and $x^* = \frac{\mu - \gamma\epsilon - 1}{\mu - \gamma\epsilon}$.

Spatiotemporal intermittency can be found at many points in the parameter space, unlike the homogeneous logistic coupled map lattice, where STI is found for values of μ which lie near the period 3 window.

Bifurcations from the synchronised fixed points can be used to obtain indicators of regions where spatiotemporal intermittency can be found. Spatiotemporal intermittency can be seen in the vicinity of bifurcation lines of co-dimension 1 and

bifurcation points of co-dimension 2 where such lines intersect each other. It is interesting to note that pure spatial intermittency, where there are bursts interspersed with laminar behaviour on the spatial lattice, accompanied by purely temporal periodic behaviour, can be found in the vicinity of some tangent-period doubling points where the eigen-values of the stability matrix cross $+1$ and -1 at the same point in the parameter space.

These conditions are satisfied for the fixed point $x^* = 0.0$ in the neighbourhood of $\epsilon = 0.635$, $\gamma = 1.1$ where the eigen-values are -0.9127, and 1.0585 respectively. We show the spatial intermittency present in the vicinity of this point in Fig. 5. The parameter values chosen are $\gamma = 1.19$ and $\epsilon = 0.635$. The space-time plot of the system can be seen in Fig. 5. The temporal period two structure of both the laminar and burst sites can be seen clearly in the space-time plot. It is clear that the time evolution of the lattice shows stable period two oscillations at both the laminar and the burst sites. Thus the intermittency is purely spatial in nature and temporally we have stable periodic behaviour.

The temporally periodic spatial structure seen here shows the unusual occurrence of long range spatial correlations. This is reflected in the distribution of laminar lengths. The length of the laminar lengths, i.e. the number of consecutive sites which follow periodic behaviour before being interrupted by bursts is calculated. As mentioned above the spatial period in the laminar regions is two. The distribution of laminar lengths shows power-law behaviour $P(l) \approx l^{-\zeta}$ with exponent $\zeta = 1.1$.

Several other tangent-period-doubling points are also seen in this parameter space and spatial intermittency with an associated scaling exponent $\zeta = 1.1$ can be seen in their vicinity , except for the tangent-period doubling point at $\gamma = 0.66$ and $\epsilon = 0.39$ where spatiotemporal intermittency is seen (See Fig. 6(a),(b)). The distribution of laminar lengths seen here also shows power-law scaling $P(l) = l^{-\zeta_F}$ but now with exponent $\zeta_F = 2.0$. Spatiotemporal intermittency can also be seen

along lines of co-dimension 1 bifurcations along the parameter space. Here, other exponents $\zeta_2 = 1.33$ and $\zeta_3 = 1.66$ are seen. These appear to be crossover exponents.

It is interesting to note that an exponent which falls within the same range as ζ_F has been seen in the case of Rayleigh-Benard convection in an annulus [9], exponents that fall in the same range as ζ_2 have been seen for convection in a channel and for the Taylor-Dean experiment, and ζ_3 has been seen in the Chaté-Manneville CML at $r = 2.1$ and $\epsilon = 0.0045$ as well as in DP simulations [12]. Similarly the Chaté-Manneville CML at $r = 3.0$ $\epsilon_c = 0.360$ shows the exponent ζ_F. The behaviour in this model is complicated by the fact that the laminar state is periodic, and that a bifurcation to period two seems to take place very close to the bifurcation from the synchronised fixed point, therefore it is difficult to draw direct connections to behaviour seen in the earlier models. However, the model provides pointers to the following conjectures. Spatiotemporal intermittency can be found in the vicinity of bifurcations from low-ordered periodic points. The type of bifurcation that takes place as well as the nature of the stable state which precedes the bifurcation may provide an indication of the universality class of the spatiotemporal intermittency. Further work on this system could lead to interesting results.

5   Discussion

To summarise, spatiotemporal intermittency is a dynamical regime with interesting but little understood behaviour. While a plethora of phenomenological information is available on the behaviour of systems which show STI, both theoretical and experimental, a unifying picture is lacking. While the conjecture that several systems which demonstrate spatiotemporal intermittency belong to the DP universality class finds some support, further work is necessary to identify the factors which contribute to the presence or absence of DP.

The effect of travelling coherent structures on the transition to spatiotemporal intermittency deserves to be explored further, as does the connection with bifurcation behaviour. Studies of systems where the laminar state is not absorbing are few and far between. Systematic studies of such systems need to be undertaken. Further work on experimental systems is also necessary. There has been only one experiment where DP exponents have been found so far [31]. Further work also needs to be done in constructing models for the quasi-1d fluid systems which show spatiotemporal intermittency. The extent to which the behaviour seen in stochastic models like probabilistic cellular automata, is similar to the behaviour in strictly deterministic models, like those considered here, also needs to be explored further. Thus, we expect this area of research to remain active and contribute to many lively debates in the coming years.

References

[1] K. Kaneko, Prog. Theor. Phys. **58**, 112 (1987).

[2] *Theory and Applications of Coupled Map Lattices*, edited by K. Kaneko (John Wiley, England, 1993) and references therein.

[3] *Dynamical systems Approach to turbulence* by T. Bohr, M.H. Jensen, G. Paladin and A. Vulpiani, Cambridge University Press, (1998).

[4] E. Domany and W. Kinzel, Phys. Rev. Lett. **53**, 311 (1984).

[5] H. Chaté, Nonlinearity **7**,185 (1994).

[6] M. G. Zimmermann, R. Toral, O. Piro and M. San Miguel,Phys. Rev. Lett., **85**, 3612, 2000.

[7] R. Kapral, Chap. 5, pg. 135, in *Theory and applications ofcoupled map lattices* ed. by K. Kaneko, (John Wiley) (1993).

[8] F. Daviaud, M. Dubois and P. Berge, Europhys. Lett. **9**, 441(1989).

[9] S. Ciliberto and P. Bigazzi, Phys.Rev.Lett.**60**, 286 (1988).

[10] S. Bottin, F. Daviaud, O. Dauchot, and P. Manneville, Europhysics Letters, **43**, 171, (1998).

[11] M.M. Degen, I. Mutabazi and C.D. Andereck Phys.Rev. E**53** 3495 (1996).

[12] G. Colovas and C. David Andereck, Phys.Rev.E **55(3)** 2736 (1997).

[13] A. Goharzadeh and I. Mutabazi, Eur. Phys. J. B. **19**,157 (2001).

[14] S. Michalland, M. Rabaud and Y. Couder, Europhys.Lett. **22** 17 (1993).

[15] Y. Pomeau, Physica D**23**, 3 (1986).

[16] J. Rolf, T. Bohr and M.H. Jensen, *Phys. Rev. E* **57** (1998) R2503.

[17] H. Chaté and P. Manneville, Physica D **32**, 409 (1988).

[18] J.M. Houlrik, *et al*, *Phys. Rev. A* **41** 4210 (1990).

[19] P. Grassberger and T. Schreiber, *Physica D* **50**, 177 (1991).

[20] T.M. Janaki, S. Sinha and N. Gupte, Phys. Rev. E **67**, 056218 (2003).

[21] J. Gollub and S. Ramashankar, *New Perspectives in Turbulence* ed. S. Orszag and L. Sirovich, Springer, Berlin (1991).

[22] S. Nasuno and S. Kai, Europhys. Lett. **14**, 779 (1991).

[23] T. Bohr, M. van Hecke, R. Mikkelson and M. Ipsen, Phys. Rev. Lett., **86**, 5482 (2001).

[24] R. Mikkelson, M. van Hecke and T. Bohr, arXiv: cond-mat 0207208.

[25] Z. Jabeen and N. Gupte, *Phase diagram of the sine circle map lattice*, arxiv:nlin.CD/0502053.

[26] Non-universal spreading exponents are seen only for the cases where the initial state is homogeneous with symmetrically placed seeds leading to strictly symmetric spreading. However, very small departures from homogeneity are sufficient to restore the DP exponents.

[27] The sine circle map system also shows a reasonably smooth dependence of the order parameter m on ϵ when the order parameter is approached from below ϵ_c, unlike the case of the logistic map discussed in [19]. This again contributes to the appearance of DP-like behaviour in the system.

[28] R.O. Grigoriev, M.C. Cross and H.G. Schuster, Phys. Rev. Lett. **79**, 2795(1997).

[29] A. Sharma and N. Gupte, Phys. Rev. E **66**, 036210 (2002).

[30] A. Sharma and N. Gupte, International Journal of Bifurcations and Chaos, **12**, 1363 (2002).

[31] P. Rupp, R. Richter and I. Rehberg, arXiv: cond-mat/0201308.

6 Appendix

The quantities characterised by critical exponents at $\epsilon = \epsilon_c$, the critical value at which the transition to sustained spatiotemporal intermittency takes place, are :

1. The static exponents:

   (a) The escape time, τ, i.e. the time taken by the system, starting from a random initial state, to reach the absorbing state, shows power law behaviour of the form $\tau \sim L^z$.

   (b) The order parameter m, i.e. the fraction of turbulent sites, scales as $m(\epsilon_c, L, t) \sim (\epsilon - \epsilon_c)^\beta$, for $\epsilon > \epsilon_c$, at fixed t.

   (c) For $t \ll \tau$, $m(\epsilon_c, L, t) \sim t^{-\beta/\nu z}$, where ν is the correlation length exponent in space.

   (d) The correlation function $C_j(t)$ is defined as

   $$C_j(t) = \frac{1}{L} \sum_{i=1}^{L} < x_i(t)x_{i+j}(t) > - < x_i(t) >^2 \tag{7}$$

   where $x_i(t)$ is the variable value at site i at time t. The brackets denote averaging over different initial conditions. This quantity scales as $C_j(t) \sim j^{1-\eta'}$.

   (e) These bulk exponents satisfy the hyperscaling relation $2\beta/\nu = 2 - d + \eta'$.

2. When the turbulent seeds spread in an absorbing lattice, the quantities associated with the spreading exponents are :

   (a) $N(t)$, the number of active sites at time t. This scales as $N(t) \sim t^\eta$,

   (b) $P(t)$, the survival probability, or the fraction of initial conditions which show a non-zero number of active sites at time t, which shows scaling behaviour of the form $P(t) \sim t^{-\delta}$.

(c) $R^2(t)$, the mean squared deviation of the position of the active sites from the original sites of turbulent activity, averaged over the surviving runs alone.This scales as $R^2(t) \sim t^{z_s}$

r	ϵ_c	z	β	$\beta/\nu z$
2.2	0.0195(2)	1.58(2)	0.28(1)	0.16(1)
3.0	0.5870(3)	1.60(3)	0.28(1)	0.15(2)
DP		1.57	0.28	0.16

Table 1: The critical exponents of the asynchronously updated Chaté-Manneville coupled map lattice. The last row shows the corresponding DP exponents.

r	b	ϵ_c	z	$\beta/\nu z$
3.0	-0.1	0.35203(1)	1.52(3)	0.02(2)
	0.0	0.35984(3)	1.42(2)	0.18(1)
	0.2	0.37323(1)	1.58(1)	0.16(1)
DP			1.58074	0.15947

Table 2: The critical exponents of the extended 2 dimensional Chaté Manneville CML for different values of b. $b = 0.2$ shows exponents closer to the DP exponents.

k	Ω	ϵ	z	β	ν	η'
1	0.068	0.63775	1.580	0.28	1.10	1.49
1	0.064	0.73277	1.591	0.28	1.10	1.50
3.1	0.18	0.70100	1.597	0.26	1.12	1.50
3.1	0.19	0.65612	1.591	0.28	1.10	1.49
DP			1.58	0.28	1.10	1.51

Table 3: Critical static exponents of the synchronously updated coupled circle map lattice for 4 critical points. The first two critical points correspond to transitions to an unique absorbing case, while the third and fourth points correspond to weakly chaotic absorbing states. The last row shows the corresponding exponents of directed percolation.

k	Ω	ϵ	η	δ	z_s
1	0.068	0.63775	0.292	0.153	1.243
1	0.064	0.73277	0.302	0.158	1.259
3.1	0.18	0.70100	0.310	0.157	1.272
3.1	0.19	0.65612	0.308	0.156	1.251
DP			0.313	0.159	1.26

Table 4: Spreading exponents of the synchronously updated coupled circle map lattice for 4 critical points. Two active seeds in an absorbing configuration is used as initial condition. For the first 2 critical points there exists an unique absorbing state, while for the third and fourth points one can have many different absorbing states and consequently many different initial absorbing backgrounds. However we notice that the exponents obtained are the same for different initial preparations and thus appear universal for 2 active seeds. The last row shows the corresponding exponents of directed percolation.
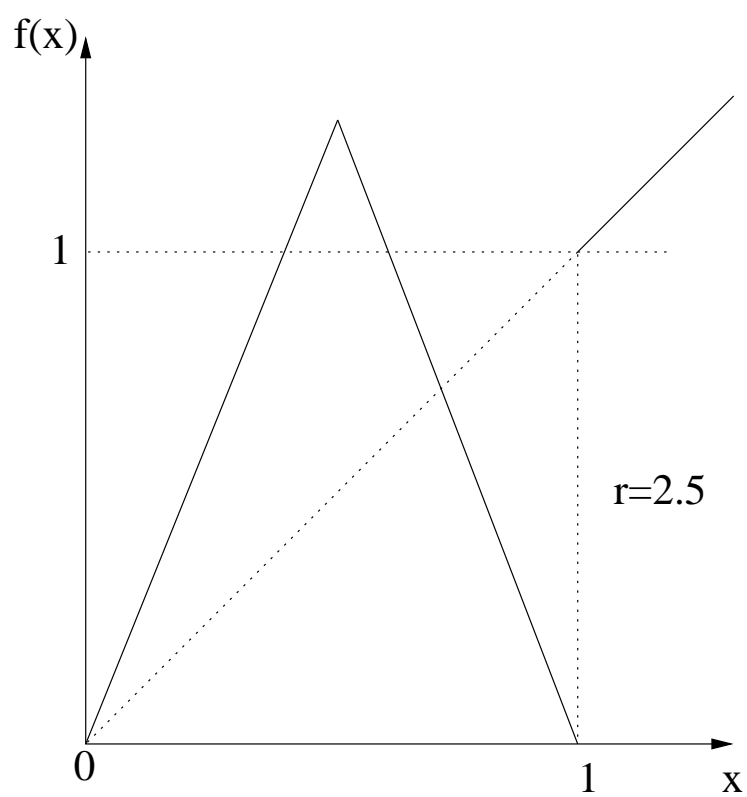
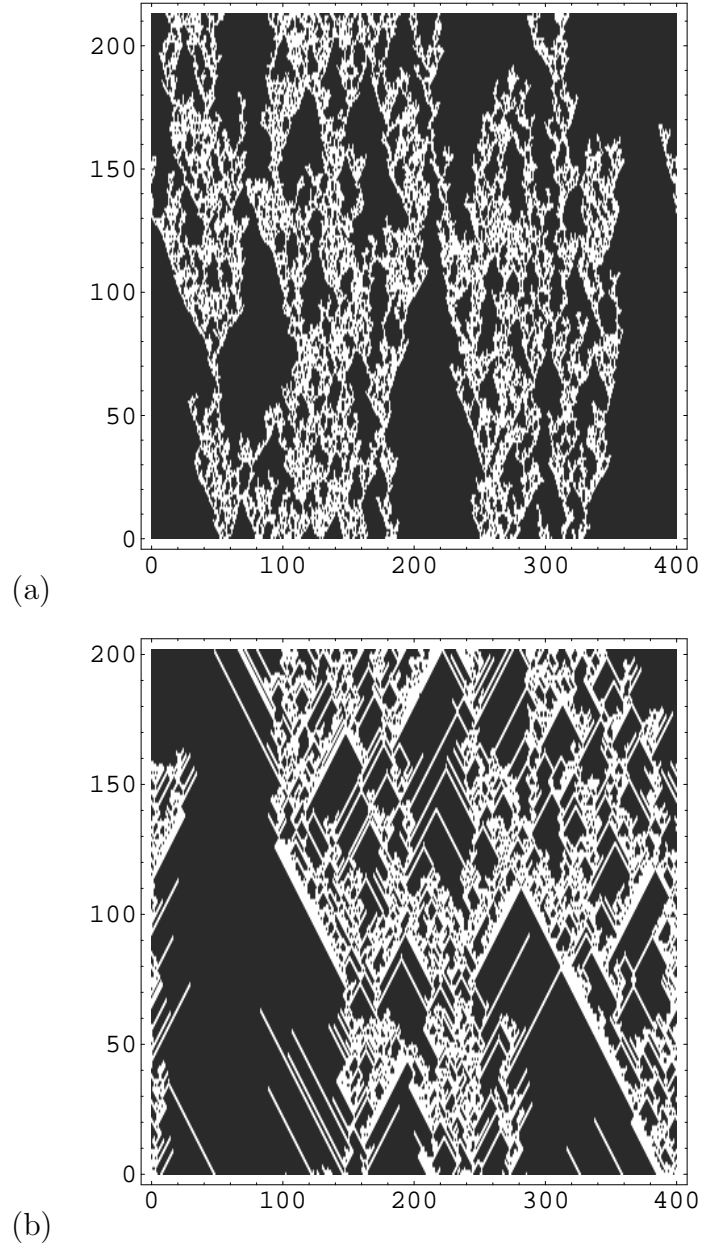Figure 1: The Chaté-Manneville map at $r = 2.5$

Figure 2: The spacetime plots for the Chaté-Manneville map for (a) $r = 2.1$, $\epsilon_c = 0.0045$ and (b) $r = 3.0$, $\epsilon_c = 0.36$ after discarding 3200 transients. Laminar sites are the black spaces. In (a), every 8th timestep has been plotted. The slower dynamics at $r = 2.1$ can be seen from the plot. Also, the solitons are clearly seen in (b).
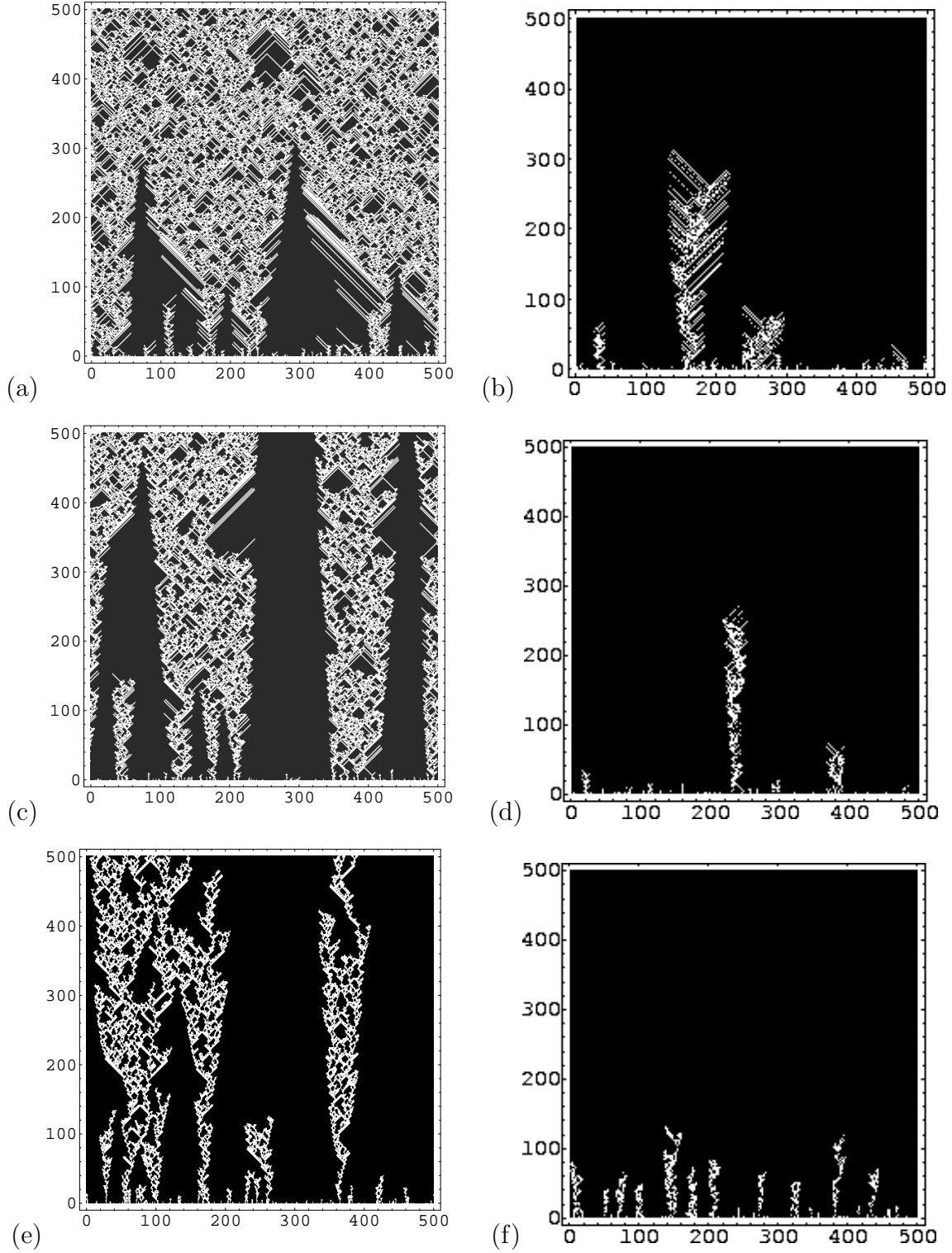
Figure 3: Space-time plots at points above (left column) and below (right column) criticality for the 2 dimensional Chaté-Manneville map for different values of b. (a) $b = -0.1$, $\epsilon = 0.359$, (b) $b = -0.1$, $\epsilon = 0.3537$, (c) $b = 0.0$, $\epsilon = 0.370$, (d) $b = 0.0$, $\epsilon = 0.365$, (e) $b = 0.2$, $\epsilon = 0.392$, (f) $b = 0.2$, $\epsilon = 0.384$. Solitons are seen at
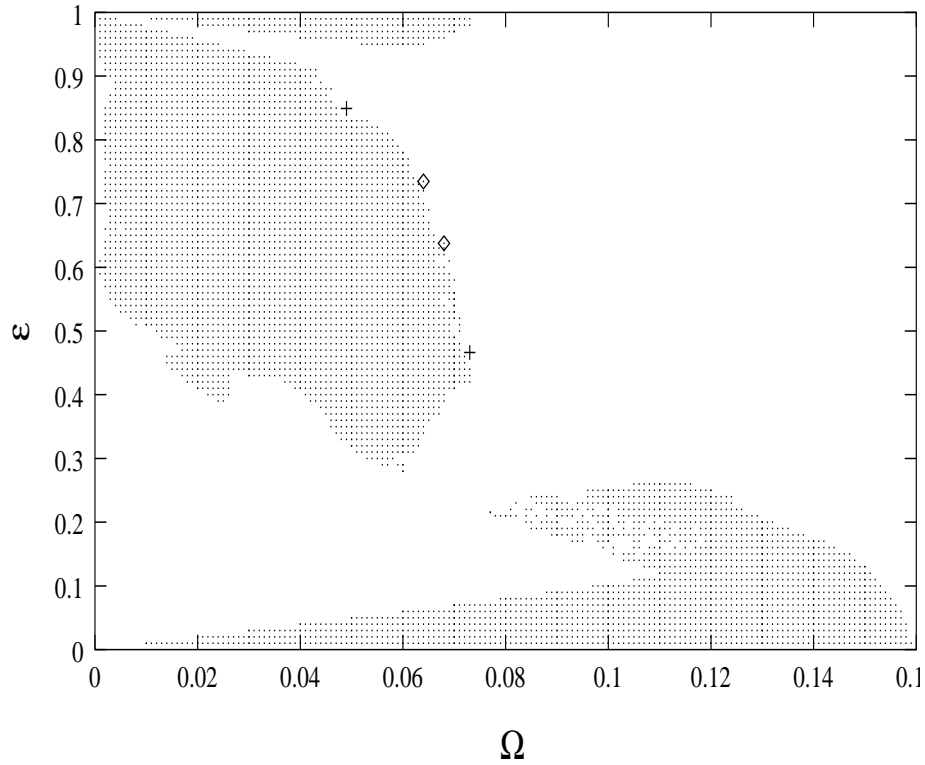
Figure 4: The phase diagram in (ϵ, Ω) space for the coupled circle map lattice at $K = 1$ after discarding 15000 transients for a lattice of 1000 sites. Random initial conditions were used. The regimes where spatially synchronised and temporally fixed solutions are obtained are shown by dots. The points at which DP-like exponents are obtained are marked by $\diamond$ [20] and $+$ [25].
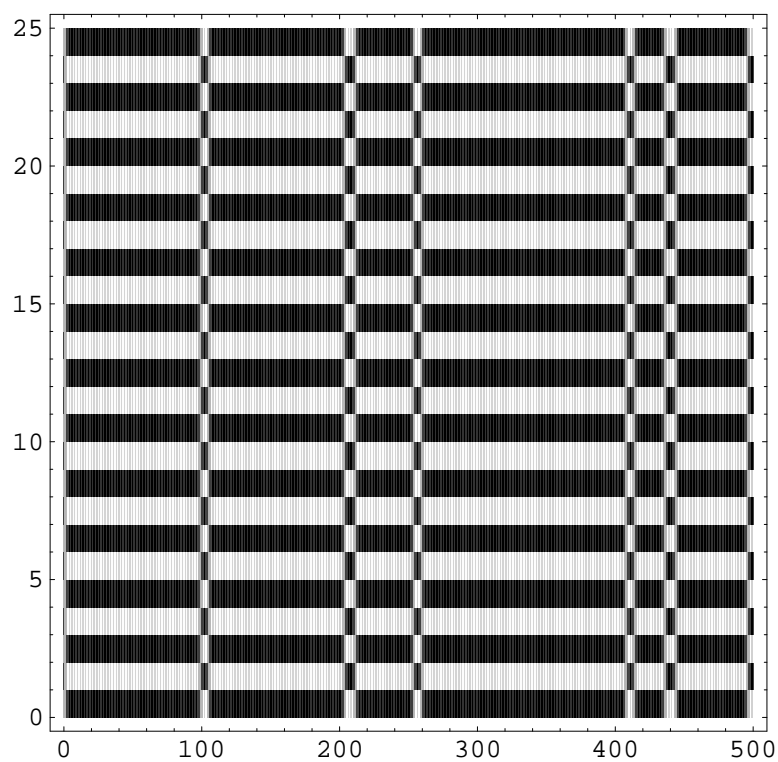
Figure 5: Spacetime plot of the inhomogenously coupled logistic map at $\gamma = 1.19$ and $\epsilon = 0.635$ for a system of 500 sites. The last 25 iterations are shown after discarding 5000 transients. Pure spatial intermittency, where the laminar region is temporally periodic is seen.
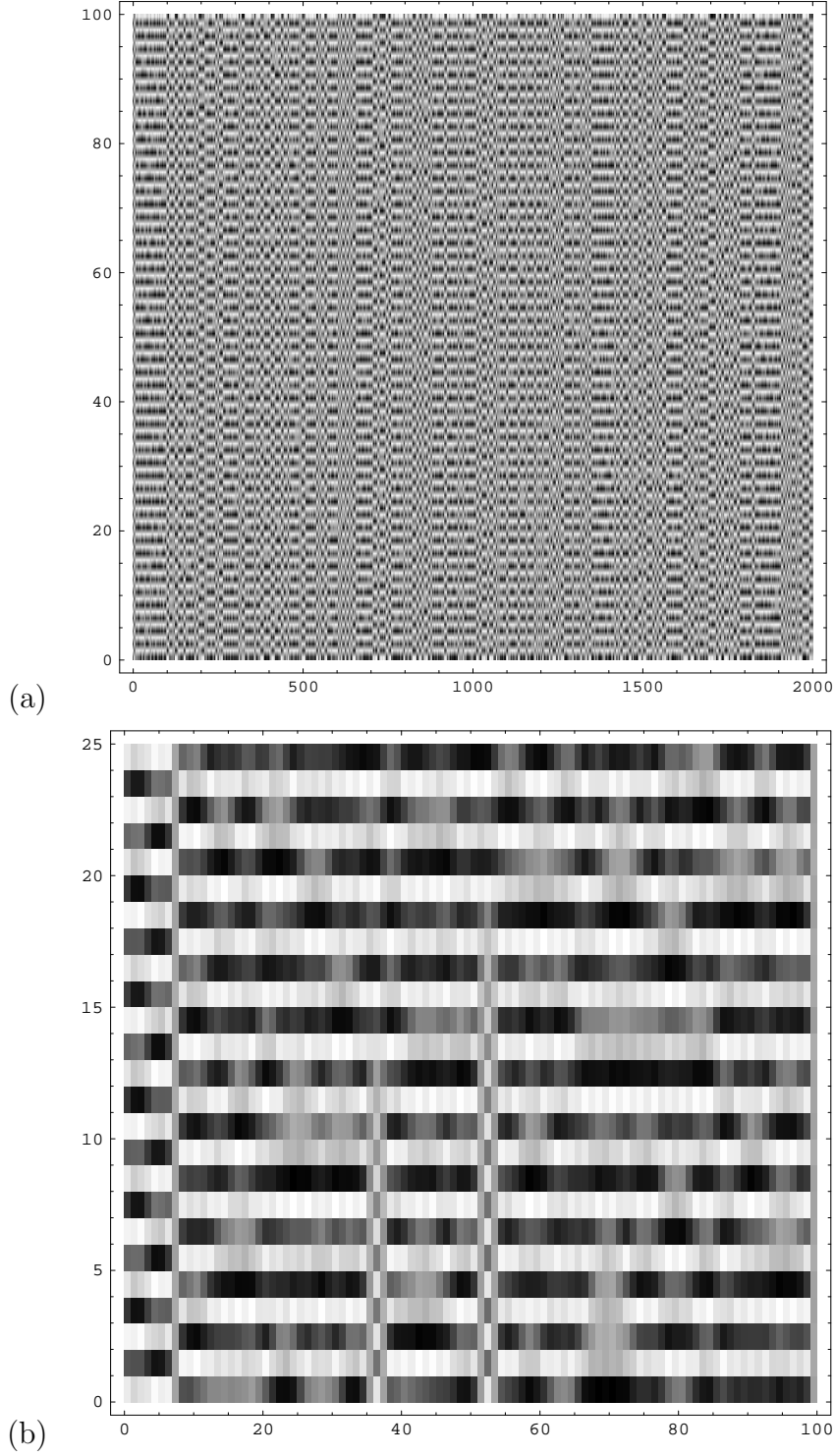
Figure 6: Spatiotemporally intermittent behaviour seen in the inhomogenously coupled logistic map at $\gamma = 0.66$ and $\epsilon = 0.39$. (a) $L = 2000$, last 100 iterations are shown after discarding $20,000$ transients. (b) $L = 500$. The last 25 iterations are shown after discarding 5000 transients.